Mechanisms of drug solubilization by polar lipids in biorelevant media

Vladimir Katev, Zahari Vinarov [*], Slavka Tcholakova

Department of Chemical and Pharmaceutical Engineering, Faculty of Chemistry and Pharmacy, Sofia University, 1164 Sofia, Bulgaria

ARTICLE INFO

ABSTRACT

Despite the widespread use of lipid excipients in both academic research and oral formulation development, rational selection guidelines are still missing. In the current study, we aimed to establish a link between the molecular structure of commonly used polar lipids and drug solubilization in biorelevant media.

The solubilization of fenofibrate by 13 phospholipids, 11 fatty acids and 2 monoglycerides was studied by an *in vitro* model of the upper GI tract. The main trends were verified with progesterone and danazol. It was revealed that to alter drug solubilization in biorelevant media, the polar lipids must form mixed colloidal aggregates with the bile. Such aggregates are formed when: (1) the polar lipid is used at a sufficiently high concentration (relative to its mixed critical micellar concentration) and (2) its hydrophobic chain has a melting temperature (T_m) < 37 °C. When these two conditions are met, the increased polar lipid chain length increases the drug solubilization capacity. Hence, long chain (C18) unsaturated polar lipids show best drug solubilization, due to the combination of long chain length and low T_m. Polar lipids with T_m significantly higher than 37 °C (*e.g.* C16 and C18 saturated compounds) do not impact drug solubilization in biorelevant media, due to limited association in mixed colloidal aggregates. The hydrophilic head group also has a dramatic impact on the drug solubilization enhancement, with polar lipids performance decreasing in the order [choline phospholipids] > [monoglycerides] > [fatty acids].

As both the acyl chain and head group types are structural features of the polar lipids, *and not of the solubilized drugs*, the described trends in drug solubilization should hold true for a variety of hydrophobic molecules.

1. Introduction

Modern drug discovery pipelines prioritize lipophilic targets (Keserü and Makara, 2009), resulting in new drug candidates with poor solubility in water (Benet et al., 2011). The slow and incomplete dissolution of such drugs in the human gastro-intestinal (GI) fluids is one of the factors that limits their oral absorption and bioavailability, hence challenging the development of new oral drug products (Augustijns et al., 2014; Boyd et al., 2019; de la Cruz-Moreno et al., 2017). One of the approaches to improve the oral bioavailability of poorly water-soluble drugs, which has recently reappeared on the drug delivery landscape, are the lipid-based formulations (LBF) (Bernkop-Schnürch et al., 2019; Feeney et al., 2016; Porter et al., 2007).

LBF have been used to develop at least 36 FDA-approved products (Savla et al., 2017) and are believed to enhance oral bioavailability by two main mechanisms: (1) increasing drug absorption by improving GI fluids solubilization capacity and sustaining drug supersaturation (Anby et al., 2012; Williams et al., 2013b) and (2) partially circumventing first-pass metabolism *via* the lymphatic absorption route (Porter et al.,

2007; Trevaskis et al., 2008). The excipient families most frequently used in LBF are glycerides (mono-, di-, tri- and their mixtures), phospholipids (PL), fatty acids (FA) and cosolvents (alcohols, PEG etc.) (Pouton, 2008). The choice of excipients and their ratios determines the dispersibility of the formulation in aqueous media, its susceptibility to digestion in the GI tract and the drug loading capacity. The LBF classification systems, which provide a link between formulation composition, dispersibility and drug solvent capacity, were introduced to rationalize the application of the concept in drug development (Pouton, 2006, 2000; Williams et al., 2014).

The dispersion of an LBF in the intestinal fluids is usually accompanied with a loss of the solubilization capacity of the carrier formulation (due to dilution and/or digestion), leading to drug precipitation, the extent of which depends on the LBF type and composition (Mohsin et al., 2009; Sassene et al., 2015; H.D. Williams et al., 2013a). The precipitation process is described by its kinetics, which defines the supersaturation window, and by the equilibrium solubility reached, which characterizes the extent of precipitation (Kaukonen et al., 2004; Kossena et al., 2004; McEvoy et al., 2017). Both the kinetic and equilibrium

---

aspects of precipitation are strongly affected by the drug solubilization capacity of the intestinal fluids, which is in turn influenced by the LBF composition. Hence, the type and concentration of excipients used in an LBF determine the drug supersaturation and precipitation behavior in the GI tract.

The behavior of LBF upon dispersion and/or digestion has been extensively studied, by using *in vitro* digestion (+ enzymes) or dispersion models (no enzymes). These models attempt to mimic the conditions in the GI tract by using one or several components encountered in the intestine (*e.g.* bile salts, phospholipids, enzymes) with widely varying levels of complexity (Berthelsen et al., 2019; Verwei et al., 2016; Williams et al., 2012). The most used digestion models are static, where the ratios of the components and the pH of the medium are constant (Brodkorb et al., 2019), as they are more accessible and easier to operate, compared to dynamic, active feedback models (MINEKUS et al., 1995). Although several standardized digestion models have been defined (Brodkorb et al., 2019; Williams et al., 2012), each is characterized by its advantages and disadvantages, and a multitude of custom digestion models are still being used (Bannow et al., 2020; Crum et al., 2016; Tran et al., 2020).

In vitro studies have demonstrated that FA, PL and glycerides generally increase drug solubilization in simulated intestinal media, with the extent of the effect being determined by the lipophilicity (Log P/D) of the drug (Christensen et al., 2004; Kleberg, 2010; Kleberg et al., 2010; Müllertz et al., 2010; Porter et al., 2007; Pouton, 2008; Rezhdo et al., 2016). However, very few studies provide a link between the structure of the excipients used and the measured drug solubilization, which hinders mechanistic understanding of drug solubilization and precipitation behavior in the intestinal environment. Kossena *et al.* showed that the solubility of hydrocortisone increases significantly with increasing the concentration of C8:0, C12:0 or C18:1 FAs in the simulated intestinal fluids (Kossena et al., 2004). It was also found that the solubilization capacity of C18:1 was much greater than that of the short-chain FAs, which was attributed to the different type of solubilizing structures formed. In another study, phosphatidylcholine was shown to have bigger effect than monoolein on the solubilization of gemfibrozil in a 10 mM sodium glycocholate solution (Luner et al., 1994). On the other hand, two studies using a design-of-experiments approach, showed that sodium oleate increases FEN solubility in biorelevant media more strongly than soy phosphatidylcholine (Dunn et al., 2019; Khadra et al., 2015). As can be seen, although significant data on LBF formulation behavior has been accumulated, there is still no clear link between excipient structure (chain length, degree of unsaturation, type of hydrophilic moiety) and drug solubilization in biorelevant media.

Therefore, we aimed to determine the relationship between the structure of several polar lipids and drug solubilization in biorelevant media. The polar lipids selected for the study include FA, PL and monoglycerides (MG): compounds that are commonly used in LBF and that are also lipid digestion products (except for the phospholipids). We investigated the effect of the length, degree of unsaturation and hydroxylation of the hydrophobic chain, as well as the effect of the hydrophilic head group type. The model compound selected for the study was fenofibrate (FEN), as an example of a drug with physicochemical properties frequently encountered in LBF development (Ditzinger et al., 2019). Experiments with progesterone (PG) and danazol (DAN) were also performed, to verify the main trends observed in the study.

2. Materials and methods

2.1. Materials

The relationship between FEN solubilization and polar lipid molecular structure was investigated by using a total of 26 lipid excipients: 13 PL, 11 FA and 2 MG. Two main groups of FA were studied: saturated FA with hydrophobic chain lengths between C8 and C18, and unsaturated FA with C18 chain and one, two or three double bonds. Two hydroxylated FA were also used: hydroxystearic acid and ricinoleic acid. In respect to MG, we studied monoolein and monostearin. A set of 13 PL with chain lengths from C10 to C18 and different hydrophilic head groups were investigated. The abbreviations and the properties of the drugs and polar lipids used are summarized in Tables 1 and 2, respectively. Methanol (99%, HPLC grade, Honeywell) was used for HPLC analysis.

The materials used for the biorelevant medium were as follows: porcine bile extract (Sigma), which contains 50 wt% bile acids (average molecular mass of 421 g/mol) (Fang et al., 2019), 6 wt% phosphatidylcholine, less than 0.06 wt% Ca^{2+} 1.2 wt% cholesterol, and 6.7 wt% FA (Z. Vinarov et al., 2012a); hydrochloric acid (36%, Sigma); NaCl (99%, Sigma); KCl (99%, Valerus); $CaCl_2$ (99%, Merck) and $NaHCO_3$ (99%, Valerus).

For gas chromatography analysis the following additional materials were used (all of purity > 99% and supplied by Sigma-Aldrich: chloroform, pyridine (anhydrous), N,O-Bis(trimethylsilyl)trifluoroacetamide (BSTFA) and isooctane.

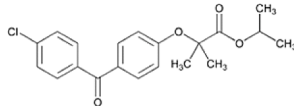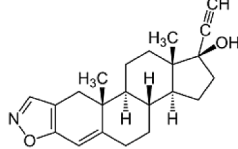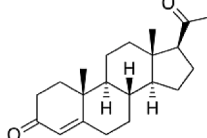### 2.2. Drug solubilization determination

2.2.1. Experiments at biorelevant conditions

Drug solubilization was determined by an *in vitro* GI tract model, which was previously used by our group to obtain useful mechanistic information about the impact of food components on lipid absorption (Vinarov et al., 2012a; Vinarova et al., 2015,2016). The concentrations of electrolytes and bile salts used are similar to the ones in the recently published INFOGEST *in vitro* digestion model (Brodkorb et al., 2019). Hence, the concentration of bile salts used (10 mM) is representative for fed state conditions (the median and mean values in post-prandial human intestinal fluids are 8 and 12 mM bile salts, respectively) (Riethorst et al., 2016).

Briefly, the protocol consists in two stages that simulate stomach and small intestinal conditions. One of the characteristic features of the model is that a physiological concentration of bicarbonate is used to gradually increase the pH in the intestinal phase from pH $\approx$ 6 to 7.5, mimicking the *in vivo* situation in the human small intestine (Maurer et al., 2015). Calcium ions are also present, which have been shown to be critical when assessing the solubilization of hydrophobic drugs and cholesterol by polar lipids, such as FA (Devraj et al., 2013; Vinarova et al., 2016).

The stomach phase was prepared by mixing 8.5 mL saline solution (59 mM NaCl, 35 mM KCl, 3.5 mM $CaCl_2$) with 6.5 mL 0.25 M HCl in a glass bottle with pre-weighted drug (45 mg FEN, 45 mg PG or 30 mg DAN) and polar lipid. The amount of polar lipid weighed corresponded to a concentration of 10 mM polar lipid at the intestinal stage (for a volume of 30 mL). Then, the sample was stirred for 30 min at the stomach conditions (pH = 2). The shift from stomach to intestinal conditions was initiated by the sequential addition of 5 mL 0.72 M $NaHCO_3$, 5 mL 2.5% porcine bile extract (pre-dissolved for 30 min at T = 37 °C) and 5 mL water (without any stirring), to obtain a final volume of 30 mL. The bottle was covered with a homemade glass cover and Teflon tape, on top of which the bottle cap was tightened. Then, the samples were stirred for 2 h. Afterwards, the bottles were opened (to facilitate the release of CO_2 and the increase of pH) and the samples were stirred for 30 min. pH $\approx$ 7 was reached at this stage. Then, the bottles were closed again and the samples were stirred for 1.5 h. At the end of the experiment, the pH of all the samples was measured (average pH of 7.5, range of 7.2 to 7.6). The total duration of the "intestinal" stage was 4 h, which mimics well the small intestinal transit time in the human GI tract, as determined by meta-analysis of trials with healthy human volunteers (3.5 h ± 1 h (Abuhelwa et al., 2016)). Temperature was kept constant at T = 37 °C, by a water bath, except one proof-of-principle experiment with DPPC, which was performed at T = 30 °C. Finally, the suspensions were filtered via 200 nm NY syringe filter to remove any

Table 1
Properties of the drugs studied.

Name and acronym used in text	Supplier, purity	M_W (g/mol)	Solubility and lipophilicity (Fagerberg *et al.*, 2015)	Structure
Fenofibrate (FEN)	TCI, 98 %	361	0.20 µg/mL LogD$_{6.5}$ = 5.3	
Danazol (DAN)	Sigma, 98 %	338	0.60 µg/mL LogD$_{6.5}$ = 3.6	
Progesterone (PG)	TCI, 98 %	315	11.18 µg/mL LogD$_{6.5}$ = 3.8	

undissolved drug particles. The filtrates were analyzed by HPLC-UV either directly, or after dilution in methanol. The experimental protocol and the final concentrations of all components are schematically illustrated in Fig. 1.

All single concentration experiments were performed in triplicate. The concentration-dependent drug solubilization by FA and MG was determined in duplicate.

2.2.2. Experiments in blank biorelevant media

To facilitate mechanistic analysis of the results, several experiments were performed in blank biorelevant media. This media had the same composition, as described in Fig. 1, without the addition of porcine bile extract. Exactly the same protocol as the one depicted in Fig. 1, was followed.

2.3. HPLC analysis of drug solubilization

HPLC analysis was carried out on a Shimadzu apparatus, equipped with two high-pressure mixing binary gradient pumps (LC-20AD), autosampler (SIL-10ADvp), four-line membrane degasser (DGU-14A), wide temperature range column oven (CTO-10ASvp) and a dual-wavelength UV–VIS detector (SPD-10Avp). We used Waters X-bridge C18 column (150 mm x 4.6 mm, 3.5 µm particle size with column guard VanGard (Waters), 3.9 mm x 5 mm - C18, 3.5 µm). The eluent flow rate was 1 mL/min and the injection volume of the sample was 20 µL. Column temperature was set at 40 °C. The concentration of solubilized drug was determined by using a standard curve (R^2 = 0.999), which was prepared by dissolving a known amount of drug in methanol. The methods used for the 3 drugs studied are summarized in Table 3.

2.4. Determination of dissolved fatty acids by gas chromatography

The fraction of dissolved FA was determined by liquid-liquid extraction, followed by derivatization and gas chromatography analysis (Vinarova et al., 2016). Briefly, the protocol consisted of the following.

The filtrate, obtained by the procedures described in section 2.2, was collected in a glass centrifuge tube (8 mL filtrate) and the pH was decreased to 2 by adding HCl. The aim of the acidification was to decrease the FA solubility in the aqueous phase. Next, 6 mL chloroform was added, and the sample was sonicated for 15 min. After every 5 min of sonication, the sample was vigorously agitated by shaking. The obtained complex dispersion was centrifuged for 30 min at $3620 \times g$ (4500 rpm) which led to separation of clear aqueous and chloroform phases.

The chloroform extracts were then derivatized by mixing 400 µL of

the sample with 100 µL internal standard (18 mg/mL hexadecanol in chloroform), 200 µL anhydrous pyridine and 200 µL N,O-Bis (trimethylsilyl)trifluoroacetamide (BSTFA). The mix was heated for 1 h at 60 °C. After cooling to room temperature, 75 µL of the sample was diluted with 950 µL isooctane in a 1.5 mL vial. The sample was then injected for gas chromatography analysis.

The gas chromatography analyses were performed on an Agilent 8890 system (Agilent technologies, USA) equipped with autosampler 7693A. We used a capillary column Agilent DB-5HT with the following specifications: (5%-Phenyl)-methylpolysiloxane, 30 m length, I.D. 0.32 mm, 0.1 µm film thickness. Cold on-column injection was used. The injection volume was 1 µL. The oven was programmed as follows: start at 60 °C, hold 1 min, the 1st ramp was to 180 °C at 10 °C/min, hold 0 min, 2nd ramp was to 375 °C at 30 °C/min, hold 10 min. The total duration of the analysis for a single sample takes 29.5 min. The flame-ionization detector (FID) temperature was set to 380 °C. The carrier gas was helium, set at a constant flow mode (2 mL/min). The detector gasses were hydrogen and air, with nitrogen as make-up gas. The secondary cooling gas was nitrogen with a purity of 99.99%. All other gasses had purity of 99.999%.

The concentration of FA and MG was calculated from the internal standard, using correction factors determined from calibration curves with standard substances.

3. Experimental results

The results for the impact of the structure of FA on drug solubilization are presented first (section 3.1), followed by the results for the effect of MG (section 3.2) and PL (section 3.3). All experiments were performed in a two-stage *in vitro* upper GI tract model, which includes 10 mM bile salts (from porcine bile extract), 1 mM Ca^{2+}, bicarbonate buffer and pH gradually increasing from 6 to 7.5 in the intestinal phase (see section 2.2 for a more detailed description).

3.1. Effect of fatty acids on drug solubilization

3.1.1. Role of fatty acid structure and concentration

The impact of 10 mM FA on the solubilization (*S*) of FEN in simulated intestinal fluids is presented in Fig. 2A. The concentration of solubilized FEN passes through a maximum as a function of the saturated FA chain length at C14:0 (myristic acid, S = 29 ±7 µg/mL), whereas the solubilizaiton by the shortest (C8:0) and longest (C18:0) FA studied was close to the control (solubilization of FEN in absence of any added FA, S = 6.5 ±0.5 µg/mL).

The effect of chain saturation and hydroxylation was studied for a

Table 2
Properties of the polar lipids studied.

Name	Acronym used in text	Supplier, purity	M_W (g/mol)	Structure
Fatty acids				
Caprylic acid	C8:0	Sigma, 99 %	144	
Capric acid	C10:0	Alfa aesar, 99 %	172	
Lauric acid	C12:0	Acros, 99 %	200	
Myristic acid	C14:0	Fluka, 98%	228	
Palmitic acid	C16:0	Sigma, 99%	256	
Stearic acid	C18:0	Across, 97 %	284	
Oleic acid	C18:1	TCI, 85 %	282	
Linoleic acid	C18:2	TCI, 91 %	280	
Linolenic acid	C18:3	TCI, 77 %	278	
Hydroxystearic acid	-	TCI, 80 %	300	
Ricinoleic acid	-	TCI, 80 %	298	
Monoglycerides				
Monostearin	-	TCI, 60 %	358	
Monolein	-	Danisco, 90 %	356	
Sodium dimyristoyl phosphatidyl glycerol	DMPG	NOF, 99 %	698	
Sodium dipalmitoyl phosphatidyl glycerol	DPPG	NOF, 99 %	745	
Sodium distearoyl phosphatidyl glycerol	DSPG	NOF, 99 %	801	
Sodium dipalmitoyl phosphatidic acid	DPPA	NOF, 99 %	670	

Table 2 (*continued*)

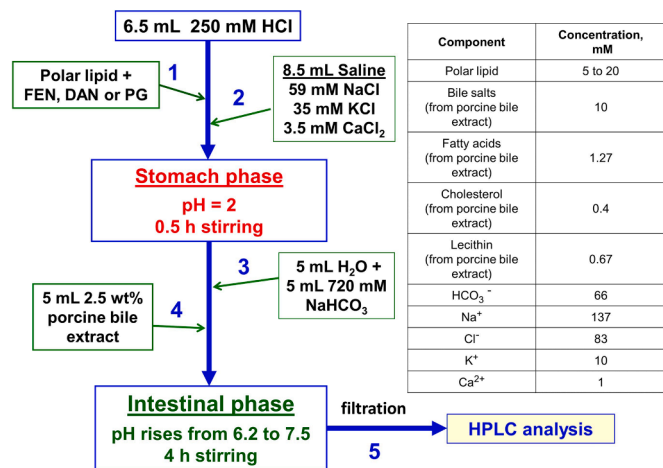| Name	Acronym used in text	Supplier, purity	M_W (g/mol)	Structure
Dipalmitoyl phosphatidyl ethanolamine	DPPE	NOF, 99 %	691	
Dipalmitoyl phosphatidyl serine	DPPS	NOF, 99 %	757	
Didecyl phosphatidyl choline	DDPC	NOF, 99 %	565	
Dilauroyl phosphatidyl choline	DLPC	Avanti, 99 %	621	
Dimiristoyl phosphatidyl choline	DMPC	Avanti, 99 %	677	
Dipalmitoyl phosphatidyl choline	DPPC	NOF, 99 %	733	
Distearoyl phosphatidyl choline	DSPC	Avanti, 99 %	789	
Palmitoleyl phosphatidyl choline	POPC	Sigma, 65 %	759	
Dioleyl phosphatidyl choline	DOPC	Avanti, 99 %	785	

Fig. 1. Schematical representation of the used two-step *in vitro* upper gastro-intestinal tract model.

Table 3
Conditions for HPLC-UV analysis of the drugs studied.

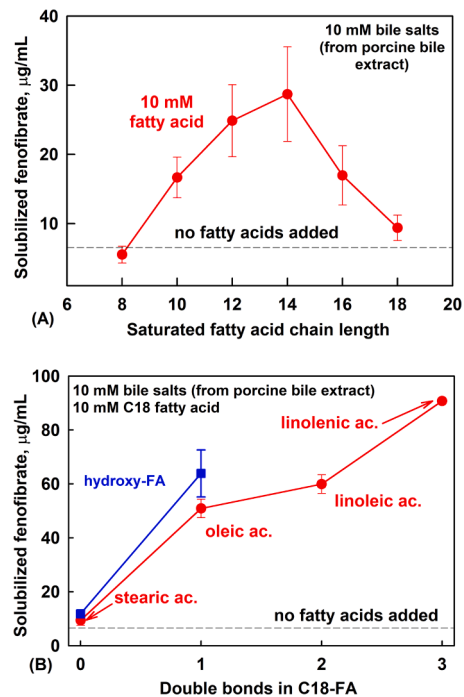| Drug	Methanol,%	Water,%	UV detection, nm	t_R, min
Fenofibrate	75	25	286	10.1
Danazol	75	25	286	5.3
Progesterone	70	30	254	7.1

Fig. 2. Solubilized fenofibrate (mean $\pm$ SD, $n = 3$) as a function of (A) the saturated fatty acid chain length or (B) the number of double bonds in C18 (red circles) or C18-OH (blue squares) fatty acids. (For interpretation of the references to colour in this figure legend, the reader is referred to the web version of this article.)

series of C18 FA homologues. The effect of the number of double bonds on FEN solubilization was non-linear (Fig. 2B): the addition of one double bond increased FEN solubilization strongly, from $S = 9 \pm 2$ µg/mL for stearic acid (C18:0) to $S = 51 \pm 3$ µg/mL for oleic acid (C18:1).

Further increase of unsaturation to two double bonds (linoleic acid) increased only slightly the solubilized FEN ($S = 59 \pm 4$ µg/mL), whereas a jump in FEN solubilization ($S = 91 \pm 1$ µg/mL) was observed when a FA with three double bonds was used (linolenic acid).

The effect of the naturally abundant hydroxy-stearic acid and hydroxy-oleic acid (ricinoleic acid) was also assessed, see the blue squares in Fig. 2B. While the hydroxylation of stearic acid increased only slightly FEN solubilization, a noticeable increase was observed when oleic acid was hydroxylated: S increased from 51 ± 3 µg/mL for C18:1 to 64 ± 9 µg/mL for C18:1-OH.

The obtained results demonstrated two interesting trends: (1) a chain length dependence that passes through a maximum and (2) a striking difference in the solubilization of FEN by saturated and unsaturated FA (note the difference in the Y-scales in Figs. 2A and 2B). To further investigate these phenomena, we studied the concentration-dependent solubilization of three hydrophobic drugs (FEN, DAN and PG) by selected saturated (C8, C10 and C18) and unsaturated FA (C18:1), see Fig. 3. For all studied drugs, it was observed that in the range of FA concentrations from 0 to 20 mM: (1) the FA with the shortest and longest chain studied (C8:0 and C18:0) have small, concentration-independent
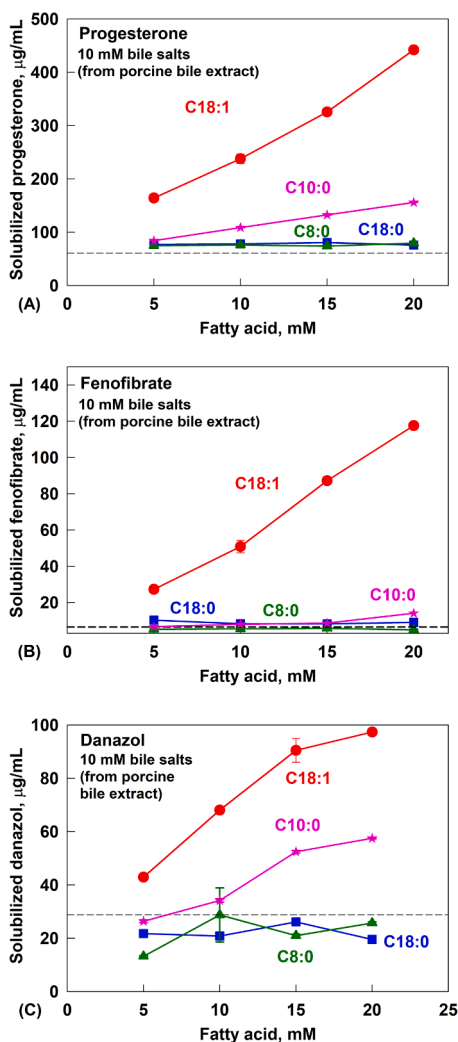

Fig. 4. Solubilization ratio (S/S_{bile}) of fenofibrate (red circles), progesterone (blue squares), or danazol (green triangles), as a function of the concentration oleic acid. Data is presented as mean $\pm$ SD, $n = 2$. (For interpretation of the references to colour in this figure legend, the reader is referred to the web version of this article.)
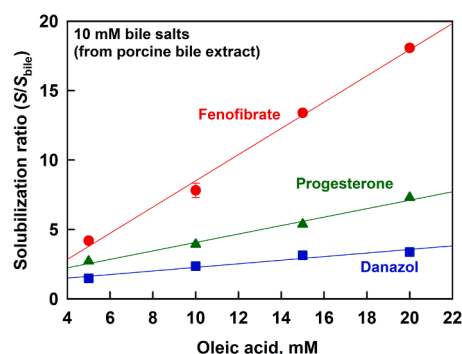
effect on drug solubilization; (2) oleic acid increases very strongly drug solubilization and (3) the C10:0 FA increases slightly, in a concentration-dependent manner, drug solubilization (the effect on FEN solubilization is visualized in Figure S1 in the Supporting information).

While the lack of effect of C18:0 FA on drug solubilization could be explained by its inability to form mixed colloidal aggregates with the porcine bile extract (discussed in section 4.2), this is not expected to be the case for the short chain C8:0 FA, which similarly did not show any effect in the range 0–20 mM. To further explore the effect of C8:0 FA, the studied concentration range was expanded with 10 additional concentrations, up to 240 mM (Figure S2 in the Supporting information). It was found that FEN solubilization was enhanced at C8:0 FA concentrations above 100 mM.

The obtained dataset can also be used to assess the effect of drug structure on solubilization by oleic acid, which showed superior performance to the saturated FA. A proper comparison between the different drugs can be achieved by using a solubilization ratio, obtained by scaling the drug solubilization in presence of oleic acid with the drug solubility in the intestinal medium in absence of additional polar lipids (S_{bile}). Such a comparison shows that oleic acid concentration had biggest effect for FEN (up to 18-fold solubilization enhancement), whereas the effect was much smaller for progesterone and danazol, see Fig. 4.

As the FA-based excipients used in drug formulation are usually composed of mixtures of FAs (*e.g.* natural fats and oils; technical FA products), we also studied FEN solubilization in binary FA mixtures at a ratio of 1:1. FA with high FEN solubilization and/or high abundance in natural fats and oils (and their derivatives) were chosen for this set of experiments: the saturated C12, C14, C16 and C18 FA, and the unsaturated C18:1 FA. Near-ideal, linear behavior ($R^2 > 0.98$) was observed for all studied pairs of FA (see Figure S4 in the Supporting information): the solubilization of FEN in the 1:1 mixtures was close or identical to the average of the individual species.

3.1.2. Dissolved fatty acids in biorelevant and blank media

The peculiar effect of FA chain length and saturation on drug solubilization (Fig. 2) prompted us to study this system in more detail. As some of the long chain FA used have very low solubility, even at conditions mimicking intestinal digestion (Vinarov et al., 2012b; Vinarova et al., 2016), it is possible that they were not completely dissolved at the concentration used for the drug solubilization experiments. Hence, we determined the concentration of *dissolved* FA in biorelevant and blank (without porcine bile extract) media. The concentration of solubilized drug (FEN) at these conditions was also quantified.

The results in the simple blank media, which lacks the solubilization power of the porcine bile extract, are in line with general expectations (Table 4): while FA with shorter chain (C8:0 and C10:0) are completely

Fig. 3. Solubilized (A) progesterone, (B) fenofibrate or (C) danazol, as a function of the concentration octanoic (green triangles), decanoic (pink stars), stearic (blue squares) and oleic acid (red circles). The dashed line represents drug solubilization at the intestinal conditions of the gastrointestinal tract model, without any added fatty acid. Data is presented as mean $\pm$ SD, $n = 2$. (For interpretation of the references to colour in this figure legend, the reader is referred to the web version of this article.)

Table 4

Dissolved fatty acids in biorelevant and blank media (no porcine bile extract), both at pH = 7.5. The concentration of solubilized fenofibrate at the same conditions is also displayed, for the purpose of comparison. The total fatty acid concentration is 10 mM. Baseline solubilization of fenofibrate in biorelevant media is 6.5 µg/mL ± 0.5 and the aqueous solubility is 0.2 µg/mL (Fagerberg et al., 2015).

Fatty acid type	Biorelevant media			Blank media (no porcine bile extract)		
	Fatty acid dissolution (%)		Fenofibrate solubilization (µg/mL)	Fatty acid dissolution (%)		Fenofibrate solubilization (µg/mL)
C8:0	100.0	±0.5	5.5 ±1.2	97.4	±0.4	N.D.
C10:0	99.3	±2.1	16.7 ±2.9	94.3	±0.3	N.D.
C12:0	92.9	±0.4	24.9 ±5.2	87.4	±0.3	8.3 ±0.3
C14:0	100.3	±1.2	28.7 ±6.9	N.D.		N.D.
C16:0	25.6	±7.3	17.0 ±4.3	N.D.		N.D.
C18:0	9.0	±0.2	9.4 ±1.8	N.D.		N.D.
C18:1	91.1	±12.6	50.9 ±3.4	N.D.		N.D.
C18:2	99.1	±1.3	59.9 ±3.5	N.D.		N.D.
C18:3	97.5	±3.9	90.71 ±0.6	N.D.		N.D.

N.D. – not detected.

dissolved (> 94%), solubility decreases with further increase of the chain length to C12:0 (87% dissolved), and all FA with 14 or more carbon atoms (including all unsaturated C18 species) are insoluble at the conditions studied. Micelles were not detected by DLS and fenofibrate was not solubilized for all FA (including the soluble C8:0 and C10:0), with the exception of C12:0, for which colloidal aggregates with Z-average around 200 nm were measured and 8.3 µg/mL ± 0.3 fenofibrate was solubilized.

However, different picture was observed in biorelevant media: the unsaturated and medium-chain FA were completely (> 90%) dissolved, while this was not the case for the long-chain palmitic and stearic acids (25.6% and 9.0% dissolved, respectively). Therefore, the concentration of FA *in solution* should be taken into account when analyzing and the impact of FA structure on drug solubilization (see section 4).

3.2. Effect of monoglycerides on drug solubilization

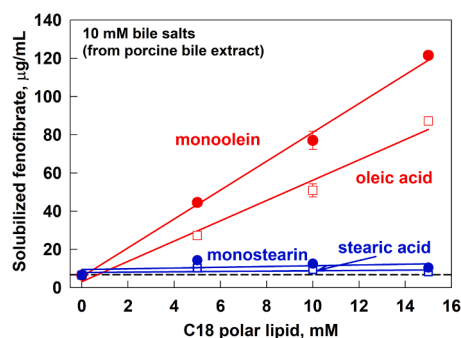We studied a MG frequently used in lipid-based formulations:

Fig. 5. Solubilized fenofibrate as a function of C18 polar lipid concentration for monoolein (full red circles), oleic acid (empty red squares), monostearin (full blue circles) and stearic acid (empty blue squares). The solid lines are a linear regression fit, whereas the dashed line represents drug solubilization at the intestinal conditions of the gastrointestinal tract model, without any added fatty acid. Data is presented as mean ± SD, n = 2. (For interpretation of the references to colour in this figure legend, the reader is referred to the web version of this article.)

monoolein (glycerol monooleate), and its saturated analogue, monostearin. The performance of these two MG was compared with the corresponding FA, see Fig. 5.

One sees that the addition of C18:1 FA or MG increases significantly FEN solubilization in a linear, dose-dependent manner. In contrast, the presence of their saturated analogues (C18:0) has a marginal effect on FEN solubilization. This striking difference between the saturated and unsaturated C18 species could be explained by their solubility in the biorelevant media used: direct measurement by gas chromatography at MG concentration of 10 mM showed that while monoolein was completely dissolved (99.4% ±0.8), only 9.3% ±0.04 of monostearin was in solution.

A comparison between monoolein and oleic acid provides further valuable information about the effect of the hydrophilic head group of the polar lipid: the slope of the dependance for monoolein was higher, compared to oleic acid. Hence, the glycerol-esterified oleic acid has significantly better performance than free oleic acid.

3.3. Effect of phospholipids on drug solubilization

The solubilization of FEN by the studied PL is presented in Fig. 6. To determine the effect of the hydrophobic chain length, we compared sets of PL with the same hydrophilic head groups (Fig. 6A): phosphatidylcholine and phosphatidylglycerol. For choline-PL, the increase of the saturated chain length from C10:0 to C16:0 leads to a gradual increase of FEN solubilization, reaching a maximum of $S = 65 \pm 5$ µg/mL. Further increase to C18:0 leads to a sharp drop in FEN solubilization, which reaches the value of the control (no PL added, $S = 6.5 \pm 0.5$ µg/mL).

In the case of the saturated phosphatidylglycerol PL, highest FEN solubilization ($S = 58 \pm 3$ µg/mL) was measured for C14:0 (DMPG). Increase of the hydrophobic chain length to C16:0 and C18:0 decreased gradually FEN solubilization, down to the control ($S = 6.5 \pm 0.5$ µg/mL).
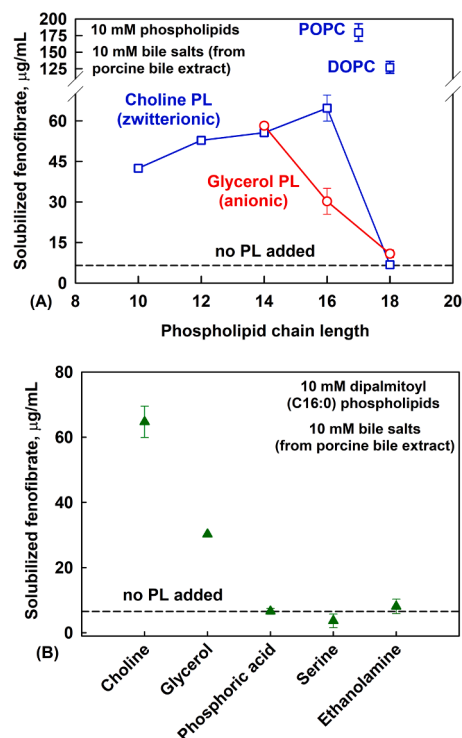
Fig. 6. Solubilized fenofibrate as a function of (A) the chain length of phosphatidylcholine (blue squares) and phosphatidylglycerol (red circles) phospholipids or (B) the hydrophilic head group type of dipalmitoyl (2 × C16:0) phospholipids. Data is presented as mean ± SD, n = 3. (For interpretation of the references to colour in this figure legend, the reader is referred to the web version of this article.)

The unsaturated DOPC and POPC showed considerably higher solubilization of FEN than all other PL studied: $S = 127 \pm 9$ and 180 ± 13 µg/mL, respectively

Next, we studied the impact of the hydrophilic moiety of the phospholipids by comparing phospholipids with the same hydrophobic chain length of C16:0 (Fig. 6B). Highest FEN solubilization was measured for phospholipids with choline head group ($S = 65 \pm 5$ µg/mL), followed by the glycerol head group ($S = 30 \pm 2$ µg/mL). All other studied head groups (phosphoric acid, serine and ethanolamine) did not enhance FEN solubilization, compared to the control ($S = 6.5 \pm 0.5$ µg/mL).

4. Discussion

4.1. The rank order of polar lipids is determined by acyl chain saturation

The studied 26 polar lipids can be arranged in three main classes, according to their FEN solubilization ratio (S/S_{Bile}), see Fig. 7: class 1, high capacity ($S/S_{bile} \geq 10$); class 2, average capacity ($10 > S/S_{bile} \geq 3$) and class 3, low capacity ($1 < S/S_{bile} < 3$). Such classification provides a framework for interesting observations: the best performing substances (class 1, $n = 4$) are unsaturated, including representatives of all classes studied (PL, FA and MG); the average performers (class 2, $n = 11$) are composed primarily of saturated compounds (PL and FA) and two unsaturated FA (C18:1 and C18:2); class 3 contains only saturated compounds ($n = 11$).

4.2. Formation of mixed colloidal aggregates

The obtained results clearly demonstrate the poor drug solubilization properties of saturated polar lipids and, in contrast, the excellent properties of long-chain unsaturated species. An obvious question to ask is what are the solubilization mechanisms that result in such clear trends, which span over some of the main classes of polar lipids (FA, MG and PL) and several poorly water-soluble drugs?

It would be reasonable to suggest that these mechanisms revolve around the ability of said polar lipids to form colloidal aggregates: whether separate or mixed with the bile salt-phospholipid colloids that originate from the porcine bile extract.

As a first step, it is useful to clarify the relative contribution of the added polar lipid to drug solubilization in the already complex biorelevant media. The studied FA could be a useful experimental set for such analysis (Table 4), which compares the drug solubilization by FA on their own (in absence of porcine bile extract) to the standard experiments (FA + bile mixtures).

Lauric acid (C12:0) was the only FA that formed colloidal aggregates in absence of porcine bile extract. However, it solubilized less than half (8.3 µg/mL ±0.3) of the FEN that was solubilized by the C12:0 + bile mixture (18.4 µg/mL ±5.2), after accounting for baseline FEN solubilization. Hence, the mixed C12:0 + bile colloidal aggregates have

significantly higher drug solubilization capacity than the separate components.

None of the other FA studied formed colloidal aggregates or solubilized FEN in absence of porcine bile extract (see section 3.1B). In contrast, the addition of most of the same FA (C10:0 to C16:0, C18:1–3) to biorelevant media increased its drug solubilization capacity (Table 4), which proves that mixed FA + bile colloidal aggregates are formed.

4.3. Short-chain polar lipids: role of solubility and CMC

However, how to explain the data for C8:0 FA, which is soluble both in blank and biorelevant media, but had no effect on drug solubilization (Table 4)? It can be suggested that the solubility of C8:0 FA is so high, that it does not form colloidal aggregates (neither separate, nor mixed with the porcine bile): hence, it does not affect drug solubilization.

For classical surfactants, the formation of colloidal aggregates is related to their CMC. One of the classical methods to determine CMC is to use a hydrophobic, water-insoluble molecule as probe (Vulliez-Le Normand and Eiselé, 1993). Hence, the concentration-dependent solubilization of the FEN and DAN by FA can be used as an indicator for the mixed CMC of the FA in biorelevant media. PG solubilization was not used for CMC determination as this drug has higher aqueous solubility and could act as a co-surfactant, which can in turn impact the CMC: a well-known effect of surface-active hydrophobic additives (Kralchevsky et al., 2003).

Hence, the solubilization of FEN was used to determine a CMC of 100 mM for C8:0 FA (see Figure S2 in the Supporting information). By using FEN and DAN solubilization, the CMCs of C10:0 (5 mM) and C18:1 FA (2 mM) were also determined (Figures S1 and S3 in the Supporting information). The CMCs of saturated FAs with chain lengths longer than C10:0 could be expected to be significantly lower than the concentration of 10 mM used in most of the experiments, as the CMC decreases 2–3 fold for each CH_2 group added to the acyl chain (Israelachvili, 2011). This gives an estimated CMC of 0.8–1.3 mM for C12:0 and 0.14–0.33 mM for C14:0.

Therefore, C8:0 FA does not enhance drug solubilization at a concentration of 10 mM, as it is below its CMC. The high solubility and the related high CMC of short-chain lipids could explain why low concentrations of C8:0 FA, C8:0 MG and their mixtures did not increase the solubilization of α-tocopherol acetate (Takahashi and Underwood, 1974) or hydrocortisone and four of its esters (Kossena et al., 2004).

4.4. Long-chain polar lipids: role of acyl chain flexibility and melting temperature

Mixed colloidal aggregate formation (or the lack of it) can also explain the drug solubilization enhancement by long chain polar lipids. For example, the small effect of stearic acid (C18:0) on drug solubilization is due to its very limited ability to form mixed colloidal
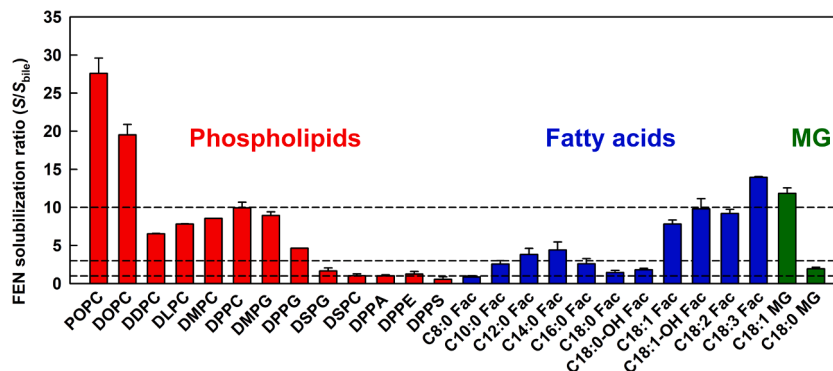

Fig. 7. Fenofibrate solubilization ratio (S/S_{bile}), as a function of polar lipid type for phospholipids (red), fatty acids (blue) and monoglycerides (green). Data is presented as mean + SD, $n = 3$. (For interpretation of the references to colour in this figure legend, the reader is referred to the web version of this article.)

aggregates with porcine bile (Table 4): only 9% of C18:0 FA were dissolved in the biorelevant media. The maximum of drug solubilization at a FA chain length of C14:0 (Fig. 2A) is also explained in the same fashion: the dissolved FA fraction decreased significantly when increasing the chain length from C14:0 to C16:0 (from 100 to 26%, respectively, Table 4). Hence, C14:0 provides optimal performance at biorelevant conditions, by balancing between high drug solubilization capacity and sufficient mixed micelle formation ability.

However, two new questions appear from this analysis: (1) why is C16 the threshold chain length for formation of bile + saturated FA mixed micelles, and (2) how come all unsaturated FA are completely incorporated in the bile micelles, despite their C18 chain (Table 4)?

The answer could be related to the molecular packing constrains inside colloidal aggregates. Long and saturated acyl chains have very limited flexibility and may be difficult to incorporate in the confined structure of the micelle, which might not be the case for the more flexible unsaturated species. Indeed, the presence of only one double bond in the acyl chain can impact considerably the packing of the molecules, as elucidated by the melting point: for example, stearic acid (C18:0) melts at 69 °C compared to 13 °C for oleic acid (C18:1).

To test this hypothesis, the solubilization ratio (S/S_{bile}) of FEN was plotted as function of the melting temperature of C18 FA with different number of double bonds (Fig. 8). The solubilization ratio was calculated by scaling the solubilization of FEN in media with added C18 FA by the baseline FEN solubilization (no polar lipids added).

Indeed, Fig. 8 shows that a reasonable correlation is obtained between these two parameters, confirming the impact of packing in the colloidal aggregates for drug solubilization (Vinarov et al., 2020). To further support the role of acyl chain flexibility, the *acyl chain* melting points of the studied FA, MG and PL were collected from the literature (Table 5). For the FA, the Krafft temperature of sodium fatty acid soaps was used for the acyl chain transition temperature. Krafft temperature is defined as the temperature of a soap solution above which colloidal aggregates are formed (McBain and Sierichs, 1948). Note that the fatty acids added to the biorelevant media (final pH = 7.5) should be in their ionized form.

The collected data confirms that palmitic acid (C16:0) has an acyl chain melting point near the temperature of the experiments ($T_{exp} = 37$ °C), which explains its limited ability to form mixed aggregates with porcine bile (Table 4) and its low impact on drug solubilization. The small or no effect of stearic acid, monostearin and all stearate-based PL on drug solubilization can be rationalized in the same way (Table 5): the acyl chain melting temperature of these polar lipids is significantly above T_{exp}, which limits the formation of mixed aggregates with the porcine bile.
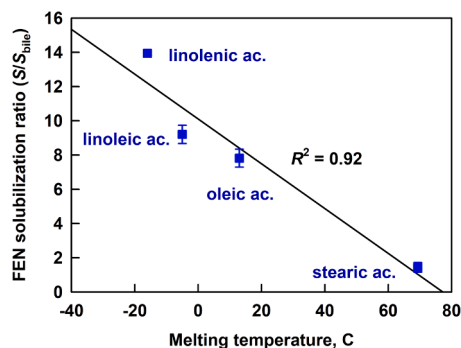
Table 5
Acyl chain phase transition temperatures of fatty acids, monoglycerides and phospholipids.

Fatty acid sodium soaps (McBain and Sierichs, 1948)		Phospholipids (Cevc, 2018)	
Type	T_m, °C	**Type**	T_m, °C
C12:0	20	DDPC	< 37
C14:0	25	DLPC	< 37
C16:0	38*	DMPC	24
C18:0	50	DMPG	24
C18:1	< 20	DPPC	41
Monoglycerides		DPPG	41
		DSPC	54
Type	T_m, °C	DSPG	54
Monostearin	57 (Batte et al., 2007)	DPPS	54
Monoolein	18 (White, 1975)	DPPE	64
		DPPA	66

Interpolated based on the data for C12, C14 and C18.

4.5. Effect of polar lipid saturated chain length: a mechanistic picture

The role of polar lipid saturated chain length on drug solubilization is illustrated in Fig. 9. The following rule is obeyed for all substances across the FA, PL and MG classes: mixed colloidal aggregates have much higher drug solubilization capacity than the control (no added polar lipids). Low concentrations of polar lipids (relative to their CMC, *e.g.* C8:0 FA) or species with rigid molecular structure (all C18:0 and most of the C16:0 polar lipids) do not form mixed colloidal aggregates and, hence, do not impact drug solubilization in biorelevant media. The role of acyl chain flexibility for drug solubilization was highlighted also in our recent study on itraconazole solubilization by mixed PL-surfactant solutions (Vinarov et al., 2020).

Discrepancy is observed for the compounds with C16:0 chains (DPPC, DPPG and palmitic acid), as they all have critical transition temperatures near $T = 37$ °C (Table 5). The increase from C14:0 to C16:0 increases the solubilization capacity in the case of choline PL, whereas a significant drop in solubilization was observed for glycerol PL and FA. However, it was shown that C16:0 FA is only partly associated in mixed colloidal aggregates with the porcine bile (Table 4). To check if the mixed bile-DPPC colloidal aggregate formation can be limited by decreasing the temperature significantly below the acyl chain melting point of DPPC, a proof-of-principle experiment was performed at $T = 30$ °C. This resulted in a significant drop of the FEN solubilization ratio, from 9.9 ± 0.74 at $T = 37$ °C to 3.8 at $T = 30$ °C. Hence, the role of acyl chain mobility and acyl chain melting temperature was confirmed also for polar lipids which experience acyl chain phase transition near the
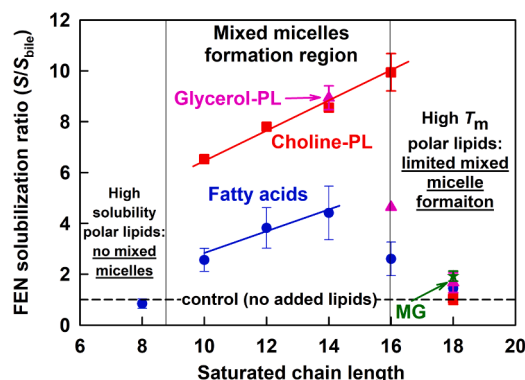

Fig. 8. Fenofibrate solubilization enhancement (S/S_{bile}), as a function of the melting temperature of C18 fatty acid homologues with varying number of double bonds. The line is a linear regression fit. Data is presented as mean $\pm$ SD, $n = 3$.

Fig. 9. Fenofibrate solubilization ratio (S/S_{bile}), as a function of the saturated acyl chain length for phospholipids (phosphatidylcholine-based, red squares; phosphatidylglycerol-based, pink triangles), fatty acids (blue circles) and monoglycerides (green triangle). The lines are a linear fit. Data is presented as mean $\pm$ SD, $n = 3$. (For interpretation of the references to colour in this figure legend, the reader is referred to the web version of this article.)

conditions of the experiment.

When the conditions for mixed micelle formation are met (sufficiently high polar lipid concentration, $T_{exp} > T_m$), the increase of saturated chain length has a *positive*, linear effect on drug solubilization (Fig. 9). In agreement with the observed trend, it was recently shown that tricaprin (C10) digests have generally a higher drug solubilization efficiency, compared to tricaprylin (C8), for a set of 16 drugs in biorelevant media (Gautschi et al., 2016). The chain length effect has also been widely documented for drug solubilization by classical surfactants in aqueous media and is explained by the decreased CMC and the bigger volume available for solubilization in colloidal aggregates (Bhat et al., 2008; Krishna and Flanagan, 1989; Ong and Manoukian, 1988; Vinarov et al., 2020, 2018c, 2018b, 2018a).

4.6. Hydrophilic head group effects

The strong effect of the polar lipid head group on drug solubilization becomes apparent when polar lipids with the identical acyl chains are compared (see Figs. 5-7 and 9). The performance of oleate derivatives decreases in the order choline-PL > MG > FA (*viz.* DOPC > monoolein > oleic acid, $S_{FEN} = 127 \pm 9$, 77 ± 5 and 51 ± 3 µg/mL, respectively). The same order is observed also for the homologue series of saturated FA and choline-PL (Fig. 9): the PL always show significantly higher drug solubilization, compared to their FA analogues.

The effect of the diverse types of head groups in the PL class was displayed in Fig. 6 and can be rationalized based on the different ability to form mixed colloidal aggregates with the porcine bile, as indicated by the differences in T_m (Table 5): choline- and glycerol-PL have the lowest T_m, and show significant drug solubilization, whereas the PL with ethanolamine, phosphoric acid and serine head groups have no effect on drug solubilization, due to $T_m > T_{exp}$. All stearate (C18:0) derivatives studied have $T_m > T_{exp}$ and do not enhance drug solubilization.

Similar rank order (PL > MG > FA) of polar lipids on drug solubilization efficiency was observed also for tocopherol solubilization in mixed bile salt + polar lipid solutions (Takahashi and Underwood, 1974). The poor drug solubilization performance of free FAs, compared to their conjugated forms (MG or PL) observed in the current study, was also shown for gemfibrozil (Luner et al., 1994) and amphotericin B (Dangi et al., 1998) by studies in mixed solutions of bile salts + polar lipids (oleic acid, monoolein and lecithin).

Therefore, the available evidence shows that the solubilization enhancement of poorly water-soluble drugs by polar lipids in biorelevant media decreases in the order PL > MG > FA.

4.7. Effect of drug structure

Drug structure can also influence the solubilization, due to the diverse molecular motifs and physicochemical properties that are common for drug substances. Based on the small set of three drugs investigated in the current paper, we can conclude only that oleic acid has bigger impact on the solubilization of the aromatic fenofibrate, compared to the steroidal danazol and progesterone molecules (Fig. 4). In this case, additional interactions (*e.g.* π-π interactions between the double bonds in the FA and the aromatic structure of FEN), might explain the observed differences.

Specific drug-solubilizer interactions can have a significant impact on drug solubilization: for example, we have recently demonstrated that electrostatic attraction between oppositely charged phospholipids and drugs (albendazole and itraconazole) can significantly enhance solubilization (Vinarov et al., 2020, 2018b). Ion-dipole interactions can also promote the increase of the solubilization capacity, as shown for ionic surfactants and progesterone (Vinarov et al., 2018a). In addition, hydrogen bonding interactions could occur between FA and weakly basic drugs (Lee et al., 2018). Thus, an expanded range of carefully selected drugs needs to be studied in order to clarify the effect of drug structure on solubilization by polar lipids.

4.8. Scope of validity of the observed trends and possible impact on oral absorption

The data presented in the current study demonstrates that the ability of the polar lipids to associate in mixed colloidal aggregates with porcine bile controls drug solubilization in biorelevant media. Mixed aggregates are formed when the polar lipid concentration (relative to its solubility) and acyl chain mobility (as indicated by the melting point) are sufficient. Both parameters relate to the ability of the polar lipids to associate in colloidal structures and are sensitive to the acyl chain length and saturation, as well as to the hydrophilic head group type (this has been described in detail in classical literature)(Israelachvili, 2011; Rosen and Kunjappu, 2012; Small, 1986).

Polar lipid acyl chain unsaturation was identified as a major driver of drug solubilization, due to the improved flexibility of unsaturated chains (as evidenced by the lower T_m), which allows long-chain polar lipids to associate in colloidal aggregates.

It should be stressed that both the acyl chain and head group type are structural features of the polar lipids, *and not* of the solubilized drugs. Therefore, it can be expected that the impact of these parameters on drug solubilization could hold for a wider span of hydrophobic molecules, than the three poorly water-soluble drugs studied in this paper.

Considering the implications of increased drug solubilization for intestinal absorption, the solubility-permeability interplay needs to be addressed. It has been shown that drug solubilization in classical surfactant micelles decreases the concentration of free drug, which decreases drug permeation and ultimately results in no cumulative effect on absorption or decreased absorption (Dahan et al., 2010; Miller et al., 2011). However, *in situ* rat perfusion studies show that the intestinal permeability of drugs solubilized in mixed bile salts + polar lipids micelles could actually be increased, rather than decreased (Dangi et al., 1998; O'Reilly et al., 1994). In this context, the permeation-enhancing effects of short- and medium-chain FA are well-known and currently being used for the delivery of macromolecules (Maher et al., 2016). Hence, systematic studies should be performed to clarify the impact of drug solubilization in mixed bile salts + polar lipids micelles on permeation.

5. Conclusions

We studied the effect of 26 polar lipids on the solubilization of the poorly water-soluble drugs fenofibrate, danazol and progesterone in a two-stage *in vitro* model of the upper GI tract. The following general trends and mechanisms of drug solubilization at biorelevant conditions were revealed:

- General trends and rank-order of polar lipids:
  - Class 1 substances ($n = 4$) provide biggest enhancement of drug solubilization (>10-fold) and are represented by unsaturated polar lipids from all species studied (PL, MG and FA)
  - Class 2 materials ($n = 11$) have an intermediate effect (3–10 fold increase) and are composed primarily (80%) of saturated polar lipids
  - Class 3 materials ($n = 11$) have very low or no effect on drug solubilization and are entirely composed of saturated compounds.
- The ability of the polar lipids to form mixed colloidal aggregates with the porcine bile components controls the drug solubilization enhancement in biorelevant media:
  - Long-chain unsaturated polar lipids associate in mixed aggregates with high drug solubilization capacity due to the double bonds which increase the flexibility of the chain.
  - Saturated polar lipids with high acyl chain melting temperature ($T_m \geq 41$ °C) do not form mixed colloidal aggregates due to their rigid chain and remain undissolved – hence, they have no impact on the drug solubilization capacity of the biorelevant media.

○ At concentrations below the mixed CMC, polar lipids do not change the drug solubilization capacity of the biorelevant media (C8:0 FA).

○ The increase of the saturated chain length for polar lipids with T_m < 41 °C and C > CMC increases the volume available for solubilization in the colloidal aggregates and enhances the solubilization capacity.

• Drug solubilization enhancement by polar lipids with the same acyl chain decreases in the order PL > MG > FA.

The presented study provides an in-depth look at the performance of polar lipid excipients widely used for poorly water-soluble drug solubilization at biorelevant conditions. The obtained mechanistic insights could be used for rational drug formulation development and thus support the modern drug discovery pipelines. Further research, which expands the set of studied drugs, includes the interplay with drug phase distribution (when an additional lipid phase is present) and considers drug permeation, is required to broaden the possible implications of the results obtained.

CRediT authorship contribution statement

Vladimir Katev: Methodology, Investigation. **Zahari Vinarov:** Conceptualization, Methodology, Supervision, Writing - original draft, Writing - review & editing, Funding acquisition. **Slavka Tcholakova:** Conceptualization, Methodology, Supervision, Writing - review & editing, Funding acquisition, Project administration.

Declaration of Conflicting Interest

None.

Acknowledgements

Supplementary materials

Supplementary material associated with this article can be found, in the online version, at doi:10.1016/j.ejps.2021.105733.

References

Abuhelwa, A.Y., Foster, D.J.R., Upton, R.N., 2016. A quantitative review and meta-models of the variability and factors affecting oral drug absorption—part ii: gastrointestinal transit time. AAPS J 18, 1322–1333. 10.1208/s12248-016-9953-7.

Anby, M.U., Williams, H.D., McIntosh, M., Benameur, H., Edwards, G.A., Pouton, C.J.H., 2012. Lipid digestion as a trigger for supersaturation: evaluation of the impact of supersaturation stabilization on the in vitro and in vivo performance of self-emulsifying drug delivery systems. Mol. Pharm. 9, 2063–2079. 10.1021/mp300164u.

Augustijns, P., Wuyts, B., Hens, B., Annaert, P., Butler, J., Brouwers, J., 2014. A review of drug solubility in human intestinal fluids: implications for the prediction of oral absorption. Eur. J. Pharm. Sci. 10.1016/j.ejps.2013.08.027.

Bannow, J., Yorulmaz, Y., Löbmann, K., Müllertz, A., Rades, T., 2020. Improving the drug load and in vitro performance of supersaturated self-nanoemulsifying drug delivery systems (super-SNEDDS) using polymeric precipitation inhibitors. Int. J. Pharm. 575, 118960. 10.1016/j.ijpharm.2019.118960.

Batte, H.D., Wright, A.J., Rush, J.W., Idziak, S.H.J., Marangoni, A.G., 2007. Phase behavior, stability, and mesomorphism of monostearin-oil-water gels. Food Biophys. 10.1007/s11483-007-9026-7.

Benet, L.Z., Broccatelli, F., Oprea, T.I., 2011. BDDCS applied to over 900 drugs. AAPS J 13, 519–547. 10.1208/s12248-011-9290-9.

Bernkop-Schnürch, A., Müllertz, A., Rades, T., 2019. Self-emulsifying drug delivery systems (SEDDS) – the splendid comeback of an old technology. Adv. Drug Deliv. Rev. 142, 1–2. 10.1016/j.addr.2019.08.002.

Berthelsen, R., Klitgaard, M., Rades, T., Müllertz, A., 2019. In vitro digestion models to evaluate lipid based drug delivery systems; present status and current trends. Adv. Drug Deliv. Rev. 10.1016/j.addr.2019.06.010.

Bhat, P.A., Dar, A.A., Rather, G.M., 2008. Solubilization capabilities of some cationic, anionic, and nonionic surfactants toward the poorly water-soluble antibiotic drug erythromycin. J. Chem. Eng. Data. 10.1021/je700659g.

Boyd, B.J., Bergström, C.A.S., Vinarov, Z., Kuentz, M., Brouwers, J., Augustijns, P., Brandl, M., Bernkop-Schnürch, A., Shrestha, N., Préat, V., Müllertz, A., Bauer-Brandl, A., Jannin, V., 2019. Successful oral delivery of poorly water-soluble drugs both depends on the intraluminal behavior of drugs and of appropriate advanced drug delivery systems. Eur. J. Pharm. Sci. 137. 10.1016/j.ejps.2019.104967.

Brodkorb, A., Egger, L., Alminger, M., Alvito, P., Assunção, R., Ballance, S., Bohn, T., Bourlieu-Lacanal, C., Boutrou, R., Carrière, F., Clemente, A., Corredig, M., Dupont, D., Dufour, C., Edwards, C., Golding, M., Karakaya, S., Kirkhus, B., Le Feunteun, S., Lesmes, U., Macierzanka, A., Mackie, A.R., Martins, C., Marze, S., McClements, D.J., Ménard, O., Minekus, M., Portmann, R., Santos, C.N., Souchon, I., Singh, R.P., Vegarud, G.E., Wickham, M.S.J., Weitschies, W., Recio, I., 2019. INFOGEST static in vitro simulation of gastrointestinal food digestion. Nat. Protoc. 10.1038/s41596-018-0119-1.

Cevc, G., 2018. Phospholipids Handbook. Phospholipids Handbook. 10.1201/9780203743577.

Christensen, J.Ø., Schultz, K., Mollgaard, B., Kristensen, H.G., Mullertz, A., 2004. Solubilisation of poorly water-soluble drugs during in vitro lipolysis of medium- and long-chain triacylglycerols. Eur. J. Pharm. Sci. 23, 287–296. 10.1016/j.ejps.2004.08.003.

Crum, M.F., Trevaskis, N.L., Williams, H.D., Pouton, C.W., Porter, C.J.H., 2016. A new in vitro lipid digestion - In vivo absorption model to evaluate the mechanisms of drug absorption from lipid-based formulations. Pharm. Res. 10.1007/s11095-015-1843-7.

Dahan, A., Miller, J.M., Hoffman, A., Amidon, G.E., Amidon, G.L., 2010. The solubility-permeability interplay in using cyclodextrins as pharmaceutical solubilizers: mechanistic modeling and application to progesterone. J. Pharm. Sci. 10.1002/jps.22033.

Dangi, J.S., Vyas, S.P., Dixit, V.K., 1998. Effect of various lipid-bile salt mixed micelles on the intestinal absorption of amphotericin-B in rat. Drug Dev. Ind. Pharm. 10.3109/03639049809082364.

de la Cruz-Moreno, M.P., Montejo, C., Aguilar-Ros, A., Dewe, W., Beck, B., Stappaerts, J., Augustijns, P., Tack, J., 2017. Exploring drug solubility in fasted human intestinal fluid aspirates: impact of inter-individual variability, sampling site and dilution. Int. J. Pharm. 528, 471–484. 10.1016/j.ijpharm.2017.05.072.

Devraj, R., Williams, H.D., Warren, D.B., Mullertz, A., Porter, C.J.H., Pouton, C.W., 2013. In vitro digestion testing of lipid-based delivery systems: calcium ions combine with fatty acids liberated from triglyceride rich lipid solutions to form soaps and reduce the solubilization capacity of colloidal digestion products. Int. J. Pharm. 10.1016/j.ijpharm.2012.11.024.

Ditzinger, F., Price, D.J., Ilie, A.R., Köhl, N.J., Jankovic, S., Tsakiridou, G., Aleandri, S., Kalantzi, L., Holm, R., Nair, A., Saal, C., Griffin, B., Kuentz, M., 2019. Lipophilicity and hydrophobicity considerations in bio-enabling oral formulations approaches – a PEARRL review. J. Pharm. Pharmacol. 10.1111/jphp.12984.

Dunn, C., Perrier, J., Khadra, I., Wilson, C.G., Halbert, G.W., 2019. Topography of simulated intestinal equilibrium solubility. Mol. Pharm. 16, 1890–1905. 10.1021/acs.molpharmaceut.8b01238.

Fagerberg, J.H., Karlsson, E., Ulander, J., Hanisch, G., Bergström, C.A.S., 2015. Computational prediction of drug solubility in fasted simulated and aspirated human intestinal fluid. Pharm. Res. 10.1007/s11095-014-1487-z.

Fang, W., Wen, X., Meng, Q., Wu, W., Everaert, N., Xie, J., Zhang, H., 2019. Alteration in bile acids profile in Large White pigs during chronic heat exposure. J. Therm. Biol. 10.1016/j.jtherbio.2019.07.027.

Feeney, O.M., Crum, M.F., McEvoy, C.L., Trevaskis, N.L., Williams, H.D., Pouton, C.W., Charman, W.N., Bergström, C.A.S., Porter, C.J.H., 2016. 50 years of oral lipid-based formulations: provenance, progress and future perspectives. Adv. Drug Deliv. Rev. 10.1016/j.addr.2016.04.007.

Gautschi, N., Bergström, C.A.S., Kuentz, M., 2016. Rapid determination of drug solubilization versus supersaturation in natural and digested lipids. Int. J. Pharm. 10.1016/j.ijpharm.2016.09.015.

Israelachvili, J.N., 2011. I ntermolecular and Surface Forces: Third Edition, Intermolecular and Surface Forces: Third Edition. 10.1016/C2011-0-05119-0.

Kaukonen, A.M., Boyd, B.J., Charman, W.N., Porter, C.J.H., 2004. Drug solubilization behavior during in vitro digestion of suspension formulations of poorly water-soluble drugs in triglyceride lipids. Pharm. Res. 10.1023/B:PHAM.0000016283.87709.a9.

Keserü, G.M., Makara, G.M., 2009. The influence of lead discovery strategies on the properties of drug candidates. Nat. Rev. Drug Discov. 8, 203–212. 10.1038/nrd2796.

Khadra, I., Zhou, Z., Dunn, C., Wilson, C.G., Halbert, G., 2015. Statistical investigation of simulated intestinal fluid composition on the equilibrium solubility of biopharmaceutics classification system class II drugs. Eur. J. Pharm. Sci. 67, 65–75. 10.1016/j.ejps.2014.10.019.

Kleberg, K., 2010. Biorelevant media simulating fed state intestinal fluids : colloid phase characterization and impact on solubilization capacity. J. Pharm. Sci. 99, 3522–3532. 10.1002/jps.

Kleberg, K., Jacobsen, J., Müllertz, A., 2010. Characterising the behaviour of poorly water soluble drugs in the intestine: application of biorelevant media for solubility, dissolution and transport studies. J. Pharm. Pharmacol. 62, 1656–1668. 10.1111/j.2042-7158.2010.01023.x.

Kossena, G.A., Charman, W.N., Boyd, B.J., Dunstan, D.E., Porter, C.J.H., 2004. Probing drug solubilization patterns in the gastrointestinal tract after administration of lipid-based delivery systems: a phase diagram approach. J. Pharm. Sci. 10.1002/jps.10554.

Kralchevsky, P.A., Danov, K.D., Kolev, V.L., Broze, G., Mehreteab, A., 2003. Effect of nonionic admixtures on the adsorption of ionic surfactants at fluid interfaces. 1. sodium dodecyl sulfate and dodecanol. Langmuir. 10.1021/la0268496.

Krishna, A.K., Flanagan, D.R., 1989. Micellar solubilization of a new antimalarial drug, β-arteether. J. Pharm. Sci. 10.1002/jps.2600780713.

Lee, Y.C., Dalton, C., Regler, B., Harris, D., 2018. Drug solubility in fatty acids as a formulation design approach for lipid-based formulations: a technical note. Drug Dev. Ind. Pharm. 10.1080/03639045.2018.1483395.

Luner, P.E., Babu, S.R., Radebaugh, G.W., 1994. The effects of bile salts and lipids on the physicochemical behavior of gemfibrozil. Pharm. Res. An Off. J. Am. Assoc. Pharm. Sci. 10.1023/A:1018967401000.

Maher, S, Mrsny, R.J., Brayden, D.J., 2016. Intestinal permeation enhancers for oral peptide delivery. Adv. Drug Deliv. Rev. 10.1016/j.addr.2016.06.005.

Maurer, J.M., Schellekens, R.C.A., Van Rieke, H.M., Wanke, C., Iordanov, V., Stellaard, F., Wutzke, K.D., Dijkstra, G., Van Der Zee, M., Woerdenbag, H.J., Frijlink, H.W., Kosterink, J.G.W., 2015. Gastrointestinal pH and transit time profiling in healthy volunteers using the IntelliCap system confirms ileo-colonic release of ColoPulse tablets. PLoS ONE. 10.1371/journal.pone.0129076.

McBain, J.W., Sierichs, W.C., 1948. The solubility of sodium and potassium soaps and the phase diagrams of aqueous potassium soaps. J. Am. Oil Chem. Soc. 10.1007/BF02645899.

McEvoy, C.L., Trevaskis, N.L., Feeney, O.M., Edwards, G.A., Perlman, M.E., Ambler, C.M., Porter, C.J.H., 2017. Correlating in vitro solubilization and supersaturation profiles with in vivo exposure for lipid based formulations of the CETP inhibitor CP-532,623. Mol. Pharm. 10.1021/acs.molpharmaceut.7b00660.

Miller, J.M., Beig, A., Krieg, B.J., Carr, R.A., Borchardt, T.B., Amidon, G.E., Amidon, G.L., Dahan, A., 2011. The solubility-permeability interplay: mechanistic modeling and predictive application of the impact of micellar solubilization on intestinal permeation. Mol. Pharm. 10.1021/mp200181v.

Minekus, m., Marteau, p., Havenaar, r., Huis in 't veld, j., 1995. A multicompartmental dynamic computer-controlled model simulating the stomach and small intestine. ATLA. Altern. to Lab. Anim.

Mohsin, K., Long, M.A., Pouton, C.W., 2009. Design of lipid-based formulations for oral administration of poorly water-soluble drugs: precipitation of drug after dispersion of formulations in aqueous solution. J. Pharm. Sci. 10.1002/jps.21659.

Müllertz, A., Ogbonna, A., Ren, S., Rades, T., 2010. New perspectives on lipid and surfactant based drug delivery systems for oral delivery of poorly soluble drugs. J. Pharm. Pharmacol. 62, 1622–1636. 10.1111/j.2042-7158.2010.01107.x.

O'Reilly, J.R., Corrigan, O.I., O'Driscoll, C.M., 1994. The effect of simple micellar systems on the solubility and intestinal absorption of clofazimine (B663) in the anaesthetised rat. Int. J. Pharm. 105, 137–146. 10.1016/0378-5173(94)90459-6.

Ong, J.T.H., Manoukian, E., 1988. Micellar solubilization of timobesone acetate in aqueous and aqueous propylene glycol solutions of nonionic surfactants. Pharm. Res. An Off. J. Am. Assoc. Pharm. Sci. 10.1023/A:1015903827042.

Porter, C.J.H., Trevaskis, N.L., Charman, W.N., 2007. Lipids and lipid-based formulations: optimizing the oral delivery of lipophilic drugs. Nat. Rev. Drug Discov. 6, 231–248. 10.1038/nrd2197.

Pouton, C.W., 2008. Formulation of lipid-based delivery systems for oral administration: materials, methods and strategies. Adv. Drug Deliv. Rev. 60, 625–637. 10.1016/J.ADDR.2007.10.010.

Pouton, C.W., 2006. Formulation of poorly water-soluble drugs for oral administration: physicochemical and physiological issues and the lipid formulation classification system. Eur. J. Pharm. Sci. 10.1016/j.ejps.2006.04.016.

Pouton, C.W., 2000. Lipid formulations for oral administration of drugs: non-emulsifying, self-emulsifying and "self-microemulsifying" drug delivery systems. European Journal of Pharmaceutical Sciences. 10.1016/S0928-0987(00)00167-6.

Rezhdo, O., Speciner, L., Carrier, R., 2016. Lipid-associated oral delivery: mechanisms and analysis of oral absorption enhancement. J. Control. Release 240, 544–560. 10.1016/j.jconrel.2016.07.050.

Riethorst, D., Mols, R., Duchateau, G., Tack, J., Brouwers, J., Augustijns, P., 2016. Characterization of human duodenal fluids in fasted and fed state conditions. J. Pharm. Sci. 105, 673–681. 10.1002/jps.24603.

Rosen, M.J., Kunjappu, J.T., 2012. Surfactants and Interfacial Phenomena: Fourth Edition, Surfactants and Interfacial Phenomena: Fourth Edition. 10.1002/9781118228920.

Sassene, P.J., Mosgaard, M.D., Löbmann, K., Mu, H., Larsen, F.H., Rades, T., Müllertz, A., 2015. Elucidating the molecular interactions occurring during drug precipitation of weak bases from lipid-based formulations: a case study with cinnarizine and a long chain self-nanoemulsifying drug delivery system. Mol. Pharm. 10.1021/acs.molpharmaceut.5b00498.

Savla, R., Browne, J., Plassat, V., Wasan, K.M., Wasan, E.K., 2017. Review and analysis of FDA approved drugs using lipid-based formulations. Drug Dev. Ind. Pharm. 10.1080/03639045.2017.1342654.

Small, D.M., 1986. The Physical Chemistry of Lipids. The Physical Chemistry of Lipids. 10.1007/978-1-4899-5333-9.

Takahashi, Y.I., Underwood, B.A., 1974. Effect of long and medium chain length lipids upon aqueous solubility of α-tocopherol. Lipids 9, 855–859. 10.1007/BF02532609.

Tran, T., Bønløkke, P., Rodríguez-Rodríguez, C., Nosrati, Z., Esquinas, P.L., Borkar, N., Plum, J., Strindberg, S., Karagiozov, S., Rades, T., Müllertz, A., Saatchi, K., Häfeli, U.O., 2020. Using in vitro lipolysis and SPECT/CT in vivo imaging to understand oral absorption of fenofibrate from lipid-based drug delivery systems. J. Control. Release 317, 375–384. 10.1016/j.jconrel.2019.11.024.

Trevaskis, N.L., Charman, W.N., Porter, C.J.H., 2008. Lipid-based delivery systems and intestinal lymphatic drug transport: a mechanistic update. Adv. Drug Deliv. Rev. 10.1016/j.addr.2007.09.007.

Verwei, M., Minekus, M., Zeijdner, E., Schilderink, R., Havenaar, R., 2016. Evaluation of two dynamic in vitro models simulating fasted and fed state conditions in the upper gastrointestinal tract (TIM-1 and tiny-TIM) for investigating the bioaccessibility of pharmaceutical compounds from oral dosage forms. Int. J. Pharm. 10.1016/j.ijpharm.2015.11.048.

Vinarov, Z., Dobreva, P., Tcholakova, S., 2018a. Effect of surfactant molecular structure on Progesterone solubilization. J. Drug Deliv. Sci. Technol. 10.1016/j.jddst.2017.09.014.

Vinarov, Z., Gancheva, G., Burdzhiev, N., Tcholakova, S., 2020. Solubilization of itraconazole by surfactants and phospholipid-surfactant mixtures: interplay of amphiphile structure, pH and electrostatic interactions. J. Drug Deliv. Sci. Technol. 10.1016/j.jddst.2020.101688.

Vinarov, Z., Gancheva, G., Katev, V., Tcholakova, S.S.S., 2018b. Albendazole solution formulation via vesicle-to-micelle transition of phospholipid-surfactant aggregates. Drug Dev. Ind. Pharm. 44, 1130–1138. 10.1080/03639045.2018.1438461.

Vinarov, Z., Katev, V., Radeva, D., Tcholakova, S., Denkov, N.D., 2018c. Micellar solubilization of poorly water-soluble drugs: effect of surfactant and solubilizate molecular structure. Drug Dev. Ind. Pharm. 44, 677–686. 10.1080/03639045.2017.1408642.

Vinarov, Z., Petrova, L., Tcholakova, S., Denkov, N.D., Stoyanov, S.D., Lips, A., 2012a. In vitro study of triglyceride lipolysis and phase distribution of the reaction products and cholesterol: effects of calcium and bicarbonate. Food Funct. 10.1039/c2fo30085k.

Vinarov, Z., Petrova, L., Tcholakova, S., Denkov, N.D., Stoyanov, S.D., Lips, A., 2012b. In vitro study of triglyceride lipolysis and phase distribution of the reaction products and cholesterol: effects of calcium and bicarbonate. Food Funct 3, 1206. 10.1039/c2fo30085k.

Vinarova, L., Vinarov, Z., Atanasov, V., Pantcheva, I., Tcholakova, S., Denkov, N., Stoyanov, S., 2015. Lowering of cholesterol bioaccessibility and serum concentrations by saponins: in vitro and in vivo studies. Food Funct 6. 10.1039/c4fo00785a.

Vinarova, L., Vinarov, Z., Tcholakova, S., Denkov, N.D., Stoyanov, S., Lips, A., 2016. The mechanism of lowering cholesterol absorption by calcium studied by using an in vitro digestion model. Food Funct 7. 10.1039/c5fo00856e.

Vulliez-Le Normand, B., Eiselé, J.L., 1993. Determination of detergent critical micellar concentration by solubilization of a colored dye. Anal. Biochem. 10.1006/abio.1993.1039.

White, S.H., 1975. Phase transitions in planar bilayer membranes. Biophys. J. 10.1016/S0006-3495(75)85795-X.

Williams, H.D., Sassene, P., Kleberg, K., Bakala-N'Goma, J.-.C., Calderone, M., Jannin, V., Igonin, A., Partheil, A., Marchaud, D., Jule, E., Vertommen, J., Maio, M., Blundell, R., Benameur, H., Carrière, F., Müllertz, A., Porter, C.J.H., Pouton, C.W., 2012. Toward the establishment of standardized in vitro tests for lipid-based formulations, part 1: method parameterization and comparison of in vitro digestion profiles across a range of representative formulations. J. Pharm. Sci. 101, 3360–3380. 10.1002/jps.23205.

Williams, H.D., Sassene, P., Kleberg, K., Calderone, M., Igonin, A., Jule, E., Vertommen, J., Blundell, R., Benameur, H., Müllertz, A., Porter, C.J.H., Pouton, C.W., 2014. Toward the establishment of standardized in vitro tests for lipid-based formulations, part 4: proposing a new lipid formulation performance classification system. J. Pharm. Sci. 10.1002/jps.24067.

Williams, H.D., Sassene, P., Kleberg, K., Calderone, M., Igonin, A., Jule, E., Vertommen, J., Blundell, R., Benameur, H., Müllertz, A., Pouton, C.W., Porter, C.J.H., 2013a. Toward the establishment of standardized in vitro tests for lipid-based formulations, part 3: understanding supersaturation versus precipitation potential during the in vitro digestion of type I, II, IIIA, IIIB and IV lipid-based formulations. Pharm. Res. 10.1007/s11095-013-1038-z.

Williams, H.D., Trevaskis, N.L., Yeap, Y.Y., Anby, M.U., Pouton, C.W., Porter, C.J.H., 2013b. Lipid-based formulations and drug supersaturation: harnessing the unique benefits of the lipid digestion/absorption pathway. Pharm. Res. 10.1007/s11095-013-1126-0.